

Solvation Effects on the Intracuster Elimination Channels in $M^+(L)_n$, where $M^+ = Mg^+$ and Ca^+ , $L = CH_3OH$, and NH_3 , and $n = 2-6$

Ka Wai Chan, Yang Wu, and Zhi-Feng Liu*

Department of Chemistry and Centre for Scientific Modeling and Computation Chinese, University of Hong Kong, Shatin, Hong Kong, China

Received: May 11, 2008; Revised Manuscript Received: June 24, 2008

The methanol and ammonia solvated Ca^+ or Mg^+ clusters are known to go through intracuster H or CH_3 eliminations which are typically switched on just below $n = 6$. By first principles calculations at the B3LYP/6-311+G** level, we have identified the transition structures, activation barriers, and energy changes in these reactions for clusters with 2–6 solvent molecules. The activation barrier is crucial to explain the previously reported experimental results. While increasing number of solvent molecules stabilizes a transition structure, the increasing presence of solvent molecules in the first solvation shell makes it difficult for the metal ion to assist the bond breaking through its interaction with the departing H atom or CH_3 group. The balance of these two factors determines whether a particular elimination channel could be switched on.

Introduction

In a previous report, we have studied the elimination channels in $M^+(L)$, where M^+ is either Mg^+ or Ca^+ , and L is either CH_3OH or NH_3 .¹ They are the first members of the corresponding solvation cluster series, $M^+(L)_n$, each of which contains a solute (the metal ion), an electron (on the singly occupied molecular orbital, SOMO), and solvent molecules.^{2–8} They are the model systems in which the solvation of the electron and the solute could lead to dramatic changes in chemical reactivity.^{9–11} Experimentally, it is known as the “size-dependent effect”: an elimination channel (such as H or CH_3 elimination in $M^+(CH_3OH)_n$)⁸ is switched on and then off as the number of solvents increases. The methanol clusters are especially interesting, because there are three possible elimination channels, H(OH) elimination by breaking the O–H bond, H(CH) elimination by breaking the C–H bond, and CH_3 elimination by breaking the C–O bond.^{7,8} The mechanisms of these reactions are now well-understood in the case of $M^+(L)$. Both the transition structures and intermediates have been carefully mapped out. The interaction between the departing atom H or group CH_3 and the metal ion varies in strength, depending on which bond is broken.¹

Significant changes are expected for these reactions as the number of solvent molecules increases beyond 1. It has been demonstrated before in the H elimination of $Mg^+(H_2O)_n$, which is probably the most studied cluster series among the solvation ionic clusters of alkaline earth metal monocations.^{12–19} The reaction, which is switched on around $n = 6$ and off around $n = 16$, has been fully elucidated. It also provides a reference for understanding the elimination channels in this report.

Watanabe et al. first made the observation that while the Mg ion in $Mg^+(H_2O)_n$ was singly charged, in the elimination product $(MgOH)^+(H_2O)_{n-1}$, the Mg ion was doubly charged.¹⁷ Successive addition of water molecules would stabilize the product $(MgOH)^+(H_2O)_{n-1}$ more than the reactant $Mg^+(H_2O)_n$, and a switch in relative stability was verified around $n = 6$ by ab initio calculations. It provided an account for the switch-on of

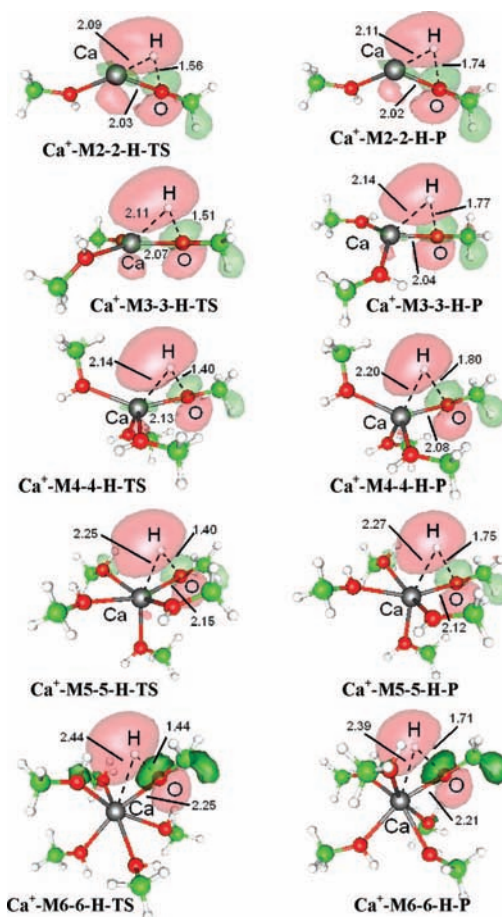


Figure 1. Transition and intermediate structures and their SOMO plots for the H(OH) elimination channel in $Ca^+(CH_3OH)_n$.

hydrogen elimination based on energy change, which has also been applied to other clusters, such as $Ca^+(H_2O)_n$ ²⁰ and $Mg^+(CH_3OH)_n$.⁸

More recent studies on the elimination mechanism have found that there is a trend of decreasing reaction barrier as the number

* To whom correspondence should be addressed. E-mail: zffiu@cuhk.edu.hk.

TABLE 1: Vertical Ionization Potentials (VIP), Charge on Ca in Reactants, O–H Distances in Transition Structures, Energy Barriers, Reaction Energies, Ca–H Distances and the Energy for H Removal in the Intermediate Structure, for the H(OH)-elimination in $\text{Ca}^+(\text{CH}_3\text{OH})_n$, $n = 2-6$, Calculated at the B3LYP/6-311+G Level^a**

	VIP (in eV)	charge on Ca	$r(\text{O}-\text{H})$ (in Å)	energy barrier	reaction energy	$r(\text{Ca}-\text{H})$ (in Å)	energy for H removal
$\text{Ca}^+-\text{M2}-2$	9.4	0.99	1.56	25.2	25.5	2.11	5.9
$\text{Ca}^+-\text{M3}-3$	8.3	1.02	1.51	16.8	16.8	2.14	5.7
$\text{Ca}^+-\text{M4}-4$	7.7	1.06	1.40	10.4	9.5	2.20	3.4
$\text{Ca}^+-\text{M5}-5$	7.2	1.10	1.40	7.7	7.5	2.27	2.3
$\text{Ca}^+-\text{M6}-6$	6.8	1.45	1.44	6.8	6.8	2.39	0.4

^a All energies are measured in kcal/mol and corrected for zero vibration.

TABLE 2: Calculated C–O Distances in Transition Structures, Energy Barriers, Reaction Energies and Energies for Removing CH_3 from the Intermediates, for the CH_3 -Elimination in $\text{Ca}^+(\text{CH}_3\text{OH})_n$, $n = 2-6$, Calculated at the B3LYP/6-311+G Level^a**

	$r(\text{C}-\text{O})$ (in Å)	energy barrier	reaction energy	energy for CH_3 removal
$\text{Ca}^+-\text{M2}-2$	2.01	21.3	-4.8	9.0
$\text{Ca}^+-\text{M3}-3$	1.93	16.7	-12.3	6.8
$\text{Ca}^+-\text{M4}-4$	1.88	12.9	-16.6	1.0
$\text{Ca}^+-\text{M5}-5$	1.83	10.4	-21.1	0.5
$\text{Ca}^+-\text{M6}-6$	1.81	10.3	-25.2	2.2

^a All energies are measured in kcal/mol and corrected for zero vibration.

of water molecules increases, which can also be explained by a similar stabilization effect for the transition structure when more water molecules are around.^{15,16} With the transition and intermediate structures mapped out, it is noted that there is little interaction between the H atom and the Mg ion, and the metal plays little assistance role in the breaking of the O–H bond.¹⁵ The reaction can also be viewed as an electron transfer process, with the unpaired electron originally residing on the metal atom being transfer to a proton produced in the acidic dissociation of water, and the stabilization of the hydroxide ion in the vicinity of a metal ion becomes the crucial factor in determining the barrier height.^{16,21}

The cluster series studied in this report, $\text{M}^+(\text{CH}_3\text{OH})_n$ and $\text{M}^+(\text{NH}_3)_n$, are similar to $\text{Mg}^+(\text{H}_2\text{O})_n$ in the valence electronic configuration.²² Broadly speaking, one would expect a similar trend of more stabilization for the elimination product with increasing number of solvent molecules. However, the substitution of the solvent water by methanol or ammonia does introduce changes to the cluster reactivities.¹ The interaction between the departing H (or CH_3) and the metal ion is more complicated and more significant. Such variations provide an interesting probe into the intricate links between solvation environment and chemical reactivities, which will be explored in the following pages.

Computational Methods

The choice of method is based on our two previous studies: one on the geometrical and electronic structures for $\text{M}^+(\text{L})_n$, with $\text{M} = \text{Mg}^+$ and Ca^+ , $\text{L} = \text{CH}_3\text{OH}$ and NH_3 , and $n = 1-6$ ²² and the other on the elimination channels of the simplest clusters with $n = 1$.¹ Systematic comparisons among post-Hartree–Fock and DFT methods, with varying basis set size, indicate that for the Mg clusters, B3LYP/6-31+G* is a very good choice between computational cost and accuracy. However, for the Ca clusters, a larger basis set is required,²² because the structures could be very sensitive to the basis sets used. All calculations are performed with the Gaussian 03 package at the B3LYP/6-

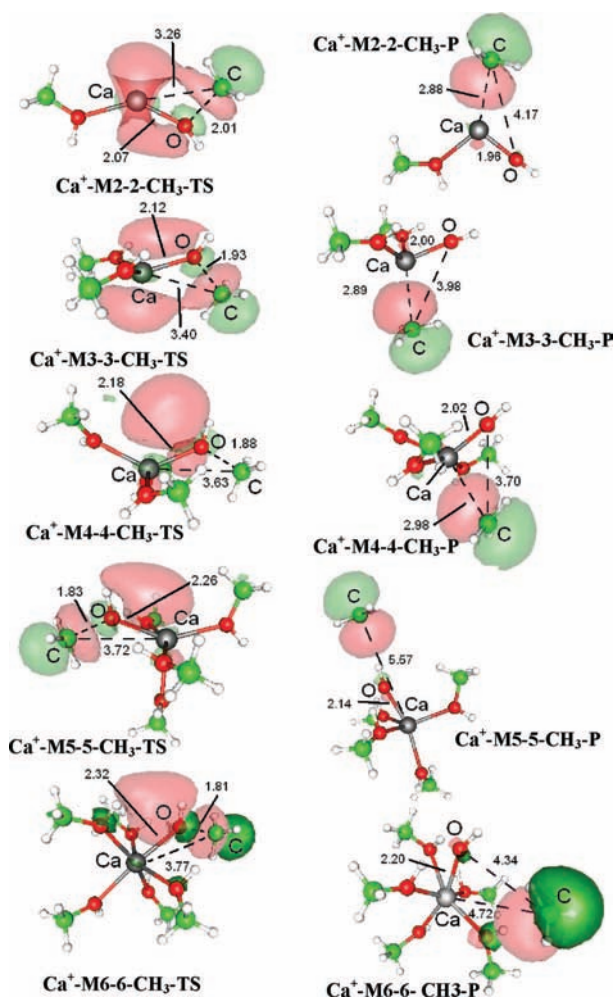


Figure 2. Transition and intermediate structures and their SOMO plots for the CH_3 elimination channel in $\text{Ca}^+(\text{CH}_3\text{OH})_n$.

311+G** level.²³ Vibrational frequencies are calculated to verify the nature of the stationary structures.

Results and Discussion

1. H(OH) and CH_3 Elimination for $\text{Ca}^+(\text{CH}_3\text{OH})_n$: Reaction Energy versus Barrier. These two reactions channels are expected to be relatively simple for two reasons. First, their structures are relatively simple. As the cluster size n increases from 2 to 6, the methanol molecules will fill the first solvation shell, due to a more spacious environment around Ca^+ (than that around Mg^+) and therefore less steric repulsion among methanol molecules.²² Second, in the case of $n = 1$, both channels are found to be similar to the H elimination in $\text{Mg}^+(\text{H}_2\text{O})_n$. The departing group, H or CH_3 , is a radical weakly bound to the Ca ion. According to natural population analysis, the Ca is almost a dication, with a charge around +1.8, while the O atom is

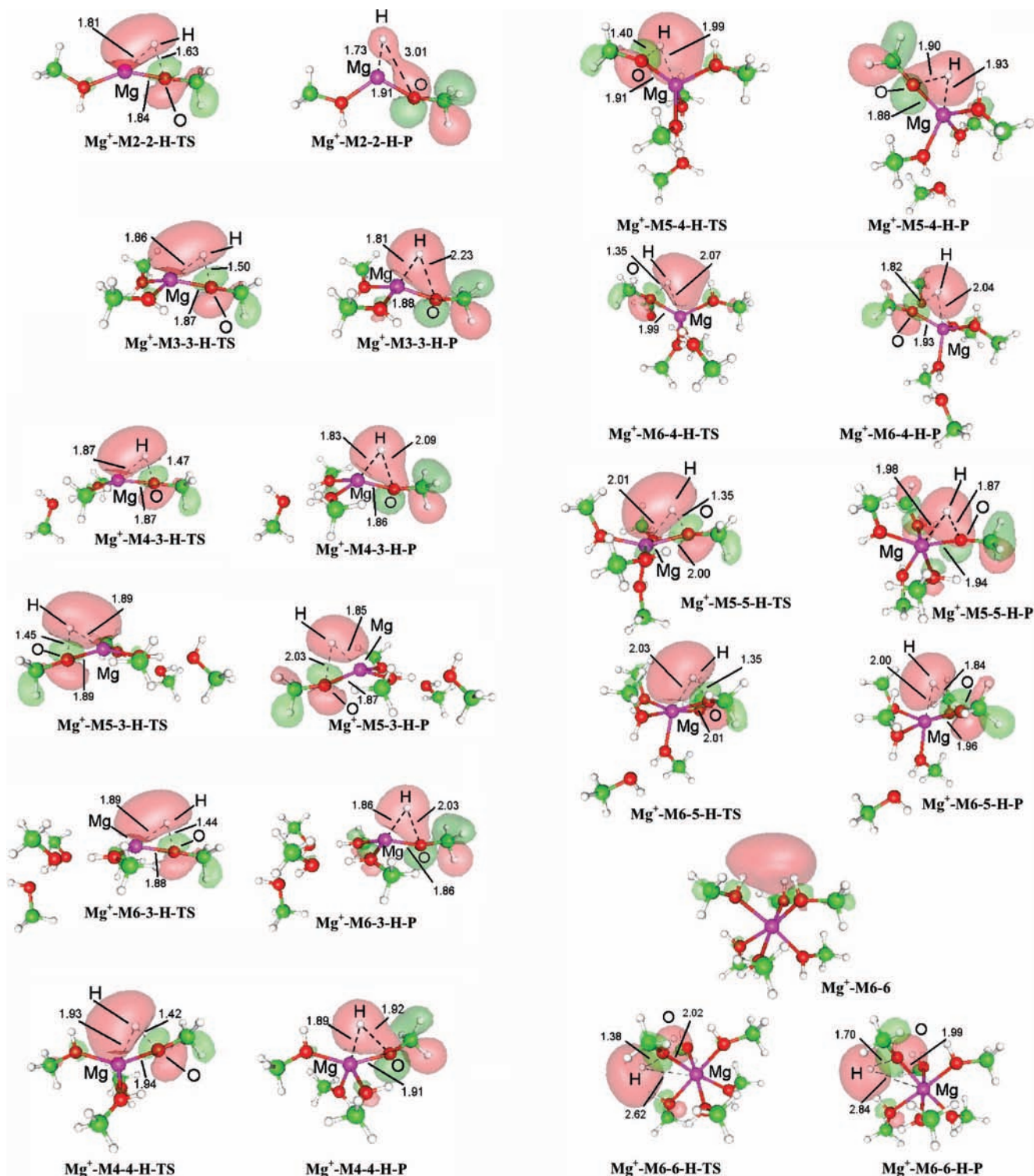


Figure 3. Transition and intermediate structures and their SOMO plots for the H(OH) elimination channel in $\text{Mg}^+(\text{CH}_3\text{OH})_n$.

negatively charged around -1.2 . It indicates that the Ca–O interaction is ionic.

For reaction energy, CH_3 elimination is actually more favorable than the H(OH) elimination, as shown in Table 1 and Table 2. CH_3 elimination becomes exothermic at $n = 2$, and reaction energy drops further with cluster size, reaching below ~ -20 kcal/mol. The same trend is observed for H(OH) elimination, although its reaction energy stays endothermic. Both trends can be easily understood by the fact that the Ca dication in the product is better stabilized by the increasing number of methanols in the larger clusters. The more favorable reaction

energy for the CH_3 elimination is also expected since the O–C bond energy (92 kcal/mol) is lower than the O–H bond energy (104 kcal/mol).²⁴

For the reaction barrier, both channels also follow the same trend of decreasing barrier with increasing cluster size. While the barrier for CH_3 elimination is lower for $n \leq 3$, the barrier for H(OH) elimination is lower for $n > 3$, although, in both cases, the difference is within a few kcal/mol.

Experimentally, both hydrogen and CH_3 elimination channels are observed around $n = 3$, and the signals for elimination products become dominant for $n \geq 4$, with the H elimination

TABLE 3: Relative Energies, Vertical Ionization Potential (VIP), Charges on Mg in Reactant, O–H Distances in Transition Structures, Energy Barriers, Reaction Energies, Mg–H Distances and Energies from Removing H from the Intermediates, for the H(OH)-Elimination in $\text{Mg}^+(\text{CH}_3\text{OH})_n$, $n = 2-6$, Calculated at the B3LYP/6-311+G Level^a**

	relative energy	VIP (in eV)	charge on Mg	$r(\text{O}-\text{H})$ (in Å)	energy barrier	reaction energy	$r(\text{Mg}-\text{H})$ (in Å)	energy for H removal
$\text{Mg}^+-\text{M2}-2$	0.0	11.2	0.98	1.63	38.2	32.7	1.73	19.2
$\text{Mg}^+-\text{M3}-3$	0.0	9.8	0.98	1.50	25.1	22.7	1.81	10.6
$\text{Mg}^+-\text{M4}-3$	0.0	9.2	0.98	1.47	22.0	19.9	1.83	9.5
$\text{Mg}^+-\text{M5}-3$	0.0	8.9	0.98	1.45	19.8	17.7	1.85	8.4
$\text{Mg}^+-\text{M6}-3$	0.0	8.6	0.98	1.44	18.1	15.8	1.86	8.1
$\text{Mg}^+-\text{M4}-4$	3.0	8.7	1.01	1.42	14.0	12.4	1.89	5.2
$\text{Mg}^+-\text{M5}-4$	0.2	7.9	1.05	1.40	11.0	9.3	1.93	4.1
$\text{Mg}^+-\text{M6}-4$	1.0	8.0	1.03	1.35	7.0	5.5	2.04	1.3
$\text{Mg}^+-\text{M5}-5$	3.5	7.7	1.08	1.35	8.3	5.9	1.98	3.0
$\text{Mg}^+-\text{M6}-5$	2.1	7.1	1.10	1.35	6.5	4.6	2.00	2.0
$\text{Mg}^+-\text{M6}-6$	0.6	6.9	1.51	1.38	6.7	6.8	2.84	0.6

^a All energies are measured in kcal/mol, and corrected for zero vibration. The relative energy is the energy difference between a particular isomer and the isomer of the same size with three solvents in the first solvation shell.

TABLE 4: C–O Distances in Transition Structures, Energy Barriers, Reaction Energies, and Energies for Removing CH_3 from the Intermediates, for the CH_3 -Elimination in $\text{Mg}^+(\text{CH}_3\text{OH})_n$, $n = 2-6$, Calculated at the B3LYP/6-311+G Level^a**

	$r(\text{C}-\text{O})$ (in Å)	energy barrier	reaction energy	energy for CH_3 removal
$\text{Mg}^+-\text{M2}-2$	2.08	30.1	8.5	15.2
$\text{Mg}^+-\text{M3}-3$	2.06	19.3	-4.5	7.7
$\text{Mg}^+-\text{M4}-3$	2.01	17.2	-5.6	5.7
$\text{Mg}^+-\text{M5}-3$	1.97	15.9	-8.6	5.2
$\text{Mg}^+-\text{M6}-3$	1.96	14.6	-10.5	5.2
$\text{Mg}^+-\text{M4}-4$	1.88	10.8	-13.6	0.6
$\text{Mg}^+-\text{M5}-4$	1.86	9.2	-16.9	0.4
$\text{Mg}^+-\text{M6}-4$	1.81	7.4	-24.5	0.7
$\text{Mg}^+-\text{M5}-5$	1.82	7.2	-23.6	2.7
$\text{Mg}^+-\text{M6}-5$	1.79	6.7	-23.7	0.2
$\text{Mg}^+-\text{M6}-6$	1.81	9.6	-24.3	1.5

^a All energies are measured in kcal/mol and corrected for zero vibration.

avored over the CH_3 elimination.⁸ Relative stability does not provide a good explanation for such observations at all. H elimination is endothermic even at $n = 6$ (6.8 kcal/mol), while CH_3 elimination becomes exothermic at $n = 2$. The elimination reactions are dissociation processes, in which products fly apart upon separation and are therefore not in a chemical equilibrium with the reactants. The experimental observations must be accounted for by the elimination barriers. By $n = 4$, the barriers for both H and CH_3 elimination have dropped to just above 10 kcal/mol, which are lower than the calculated stepwise solvation energy of 15.3 kcal/mol at $n = 4$. At this point, the elimination channels become more favorable than the loss of a solvent molecule. Furthermore, also starting at $n = 4$, the barrier for H elimination is lower than the barrier for CH_3 elimination, and therefore the former is more favored, even though it is significantly more endothermic.

2. H(OH) and CH_3 Elimination for $\text{Ca}^+(\text{CH}_3\text{OH})_n$: Transition and Intermediate Structures. Both elimination channels lead to intermediate structures, with a dangling H atom or CH_3 group. Significant changes are observed in these intermediate structures and the transition structures leading to them, as compared with the corresponding structures at $n = 1$ for $\text{Ca}^+(\text{CH}_3\text{OH})$.

In the H(OH) elimination for $\text{Ca}^+(\text{CH}_3\text{OH})$, the H atom is well separated from both the Ca and O atom. The $\text{H}\cdots\text{Ca}$ and $\text{H}\cdots\text{O}$ distances are 2.72 and 3.71 Å respectively at the B3LYP/6-311+g** level, and increase further to 2.77 and 4.27 Å in

the intermediate product.¹ In contrast, these two values are only 2.09 and 1.56 Å for the transition structure and 2.11 and 1.74 Å for the intermediate structure, in the case of $\text{Ca}^+(\text{CH}_3\text{OH})_2$. With the addition of just one more methanol, the H atom has taken up a bridge position between the Ca and O atom. As shown in Figure 1, the unpaired electron has shifted into the O–H antibonding orbital during the reaction process, while some residual density remains on Ca. As the number of methanol increases from 2 to 6, this bridge structure does not change much, although for the intermediate structure, the $\text{H}\cdots\text{Ca}$ distance increases from 2.11 Å for $n = 2$ to 2.39 Å for $n = 6$. The binding energy for the departing H is 5.9 kcal/mol at $n = 2$, and decreases gradually to 0.4 kcal/mol as n increases to 6.

For the CH_3 elimination, the changes in both the transition and intermediate structure are less significant, as compared to the case of $n = 1$. For the transition structure, the CH_3 group bridges the Ca and O atoms, with a $\text{Ca}\cdots\text{CH}_3$ distance around 3 Å and a $\text{O}\cdots\text{CH}_3$ distance around 2 Å, as shown in Figure 2. For the intermediate structure formed in the process, the $\text{O}\cdots\text{CH}_3$ distance is increased to around 4 Å, indicating little interaction between the two. On the other hand, the $\text{Ca}\cdots\text{CH}_3$ distance is below 3 Å for $n = 2$ and 3. The SOMO in the intermediate structure is a p orbital on the CH_3 radical, which can interact with Ca through a dative bond, similar to the case of $\text{Ca}^+(\text{CH}_3\text{OH})$.¹ As listed in Table 2, the energy for the complete removal of CH_3 group is 9.0 kcal/mol at $n = 2$ and 6.8 kcal/mol at $n = 3$, both larger than the corresponding value for the removal of H atom in the H(OH) elimination. However, at $n = 4$ the $\text{Ca}\cdots\text{CH}_3$ distance in the intermediate structure is increased to 3.0 Å, and there is a significant decrease in the energy for the removal of CH_3 , to merely 1.0 kcal/mol. Obviously as the first solvation shell around Ca is filled, the CH_3 group is squeezed out and is weakly bound to the rest of the cluster by van der Waals interaction Figure 3.

For both eliminations, the trend for the barrier can be well explained by the two factors previously proposed for $\text{Mg}^+(\text{H}_2\text{O})_n$.¹⁶ With increasing number in the first solvation shell, it becomes easier to push the electron over to H or CH_3 , as indicated by the decreasing ionization potential for $\text{Ca}^+(\text{CH}_3\text{OH})_n$ listed in Table 1. Furthermore, the more polarizing Ca^{2+} in the product is stabilized by the additional methanol molecules.

In addition, there is also a “squeezing-out” factor that affects the two eliminations in subtly discriminating ways. With increasing number of methanol molecules, the eliminated H or CH_3 group is pushed away from the Ca ion, as indicated by the increasing $\text{H}\cdots\text{Ca}$ and $\text{CH}_3\cdots\text{Ca}$ distance. It is not surprising

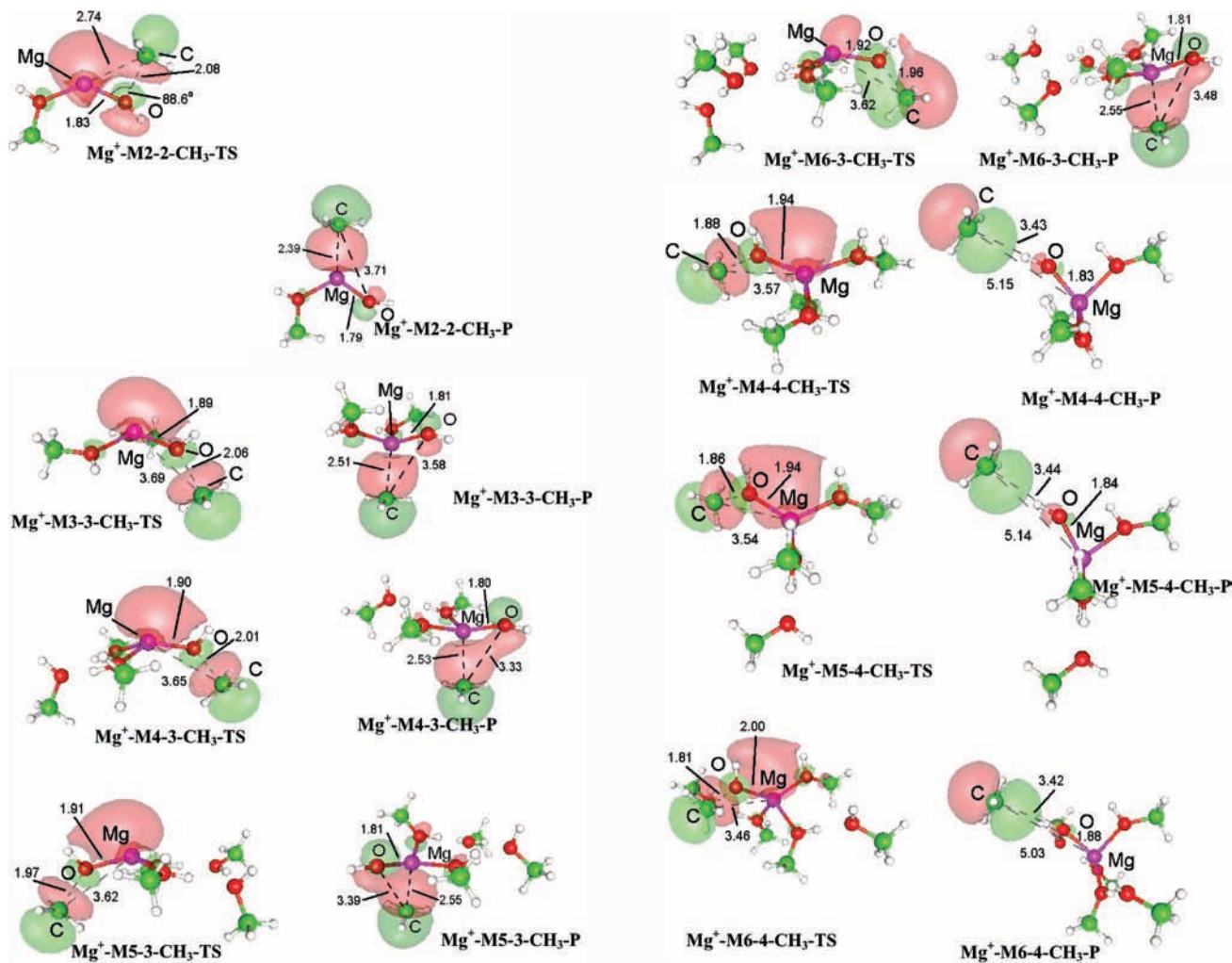


Figure 4. Transition and intermediate structures and their SOMO plots for the CH_3 elimination channel in $\text{Mg}^+(\text{CH}_3\text{OH})_n$.

that the effect is more prominent for the bulkier CH_3 group than for the H atom. Furthermore, the $\text{CH}_3 \cdots \text{Ca}$ interaction, through the singly occupied C 2p orbital, is stronger than the $\text{H} \cdots \text{Ca}$ interaction, which makes it less favorable for the CH_3 elimination. These effects provide an account for the higher barrier for CH_3 elimination than that for H (OH) elimination for $n \geq 4$, despite the fact that the O–C bond is more facile than the O–H bond.

3. H(OH) and CH_3 Elimination for $\text{Mg}^+(\text{CH}_3\text{OH})_n$. The overall trend observed for these two eliminations in the case of $\text{Mg}^+(\text{CH}_3\text{OH})_n$ is quite similar to that in the case of $\text{Ca}^+(\text{CH}_3\text{OH})_n$. Both the reaction energy and the barrier drop as the number of methanol molecules increases, as listed in Tables 3 and 4. In terms of reaction energy, CH_3 elimination is exothermic for $n \geq 3$, while H elimination is always endothermic. The barrier for CH_3 elimination is also lower than that for H elimination initially, until a switch in the ordering at $n = 6$, which is later than the switch at $n = 4$ for $\text{Ca}^+(\text{CH}_3\text{OH})_n$. The transition structures and intermediate structures are also similar for the two cluster series, with H atom or CH_3 group bridging between Mg and O, as shown in Figure 3 and Figure 4.

It should be noted that there is a significant difference between the H (OH) elimination in $\text{Mg}^+(\text{CH}_3\text{OH})$ and in $\text{Ca}^+(\text{CH}_3\text{OH})$. For $\text{Ca}^+(\text{CH}_3\text{OH})$, a H atom is produced and weakly bound to a Ca^+OCH_3 core dominated by the ionic interaction between Ca^{2+} and OCH_3^- . For $\text{Mg}^+(\text{CH}_3\text{OH})$, both the Mg and the O on OCH_3^- are less charged, while at the same time there is

significant bonding interaction between H and Mg, with a distance of 1.66 Å and a barrier of 29.3 kcal/mol to break this bond. The Mg–O interaction is less ionic in the intermediate product, which is compensated by the H–Mg interaction.¹

At $n = 2$, the H–Mg is increased to 1.73 Å in the intermediate structure $\text{Mg}^+\text{-M2-2-H-P}$, as shown in Figure 3, while the barrier to break this bond is reduced to 19.2 kcal/mol (Table 3). These numbers nonetheless indicate that significant bonding interactions remain between H and Mg. Another significant change is observed in geometry: while the H–Mg–O angle is almost 180° at $n = 1$, this angle is now bent to 111°, which is due to the presence of an additional CH_3OH . As the number of methanol in the first shell increases further, the $\text{H} \cdots \text{Mg}$ distance is lengthened. With five methanol in the first shell, this distance reaches 2 Å while the H atom dissociation barrier is reduced below 5 kcal/mol, which indicates that the $\text{H} \cdots \text{Mg}$ bond is almost broken. The hydrogen atom is gradually squeezed out from direct interaction with the Mg ion, by the presence of other methanol molecules in the first shell. It is similar to the case of CH_3 elimination in $\text{Ca}^+(\text{CH}_3\text{OH})_n$, albeit the decrease in Mg–H interaction energy is larger. It is also observed for the CH_3 elimination in $\text{Mg}^+(\text{CH}_3\text{OH})_n$, as shown in Figure 4. When the number of methanol in the first shell is less than 4, the $\text{Mg} \cdots \text{C}$ distance is below 2.6 Å. But it increases dramatically to more than 5 Å when the first shell contains 4 or more methanol molecules. Correspondingly, there is also a significant drop in the amount of energy required to

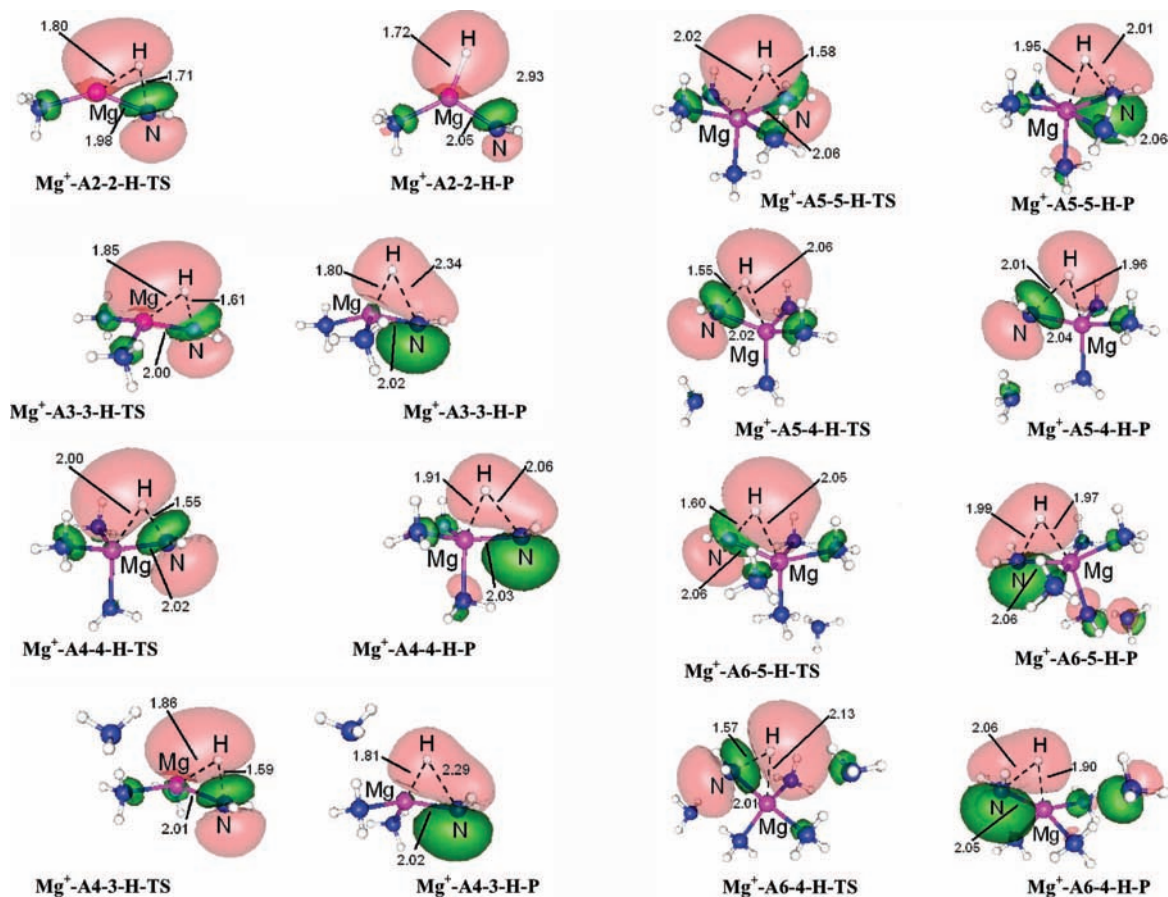


Figure 5. Transition and intermediate structures and their SOMO plots for the H elimination channel in $\text{Mg}^+(\text{NH}_3)_n$.

TABLE 5: Relative Energies, Vertical Ionization Potential (VIP), Charges on Mg in Reactants, N–H Distances in Transition Structures, Energy Barriers, Reaction Energies, Mg–H Distances and Energies for Removing H Atom from the Intermediates, for the H-Elimination in $\text{Mg}^+(\text{NH}_3)_n$, $n = 2-6$, Calculated at the B3LYP/6-311+G** Level^a

	relative energy	VIP (in eV)	charge on Mg	$r(\text{N}-\text{H})$ (in Å)	energy barrier	reaction energy	$r(\text{Mg}-\text{H})$ (in Å)	energy for H removal
$\text{Mg}^+-\text{A2}-2$	0.0	11.0	0.93	1.71	44.2	38.9	1.72	23.7
$\text{Mg}^+-\text{A3}-3$	0.0	9.5	0.93	1.61	31.6	27.8	1.80	18.4
$\text{Mg}^+-\text{A3}-2$	8.8	10.5	0.92	1.68	41.1	36.5	1.75	21.6
$\text{Mg}^+-\text{A4}-4$	0.0	7.4	1.02	1.55	22.4	20.5	1.91	11.6
$\text{Mg}^+-\text{A4}-3$	2.2	9.1	0.93	1.59	29.3	25.6	1.81	17.3
$\text{Mg}^+-\text{A5}-5$	0.0	7.1	1.05	1.58	22.3	21.3	1.95	12.0
$\text{Mg}^+-\text{A5}-4$	3.6	7.1	1.03	1.55	21.7	20.3	1.96	9.6
$\text{Mg}^+-\text{A5}-3$	6.0	8.7	0.92	1.58	27.2	23.7	1.83	16.3
$\text{Mg}^+-\text{A6}-6$	0.0	6.8	1.06					
$\text{Mg}^+-\text{A6}-5$	4.5	6.8	1.06	1.60	21.9	21.1	1.97	11.6
$\text{Mg}^+-\text{A6}-4$	7.9	6.7	1.04	1.57	20.5	18.7	1.90	9.5
$\text{Mg}^+-\text{A6}-3$	13.8	8.6	0.92					

^a All energies are measured in kcal/mol and corrected for zero vibration. The relative energy is also corrected for BSSE.

completely remove CH_3 from the intermediate structure, as listed in Table 4.

It has been shown previously that with increasing number of methanol molecules in the first solvation shell, the solute–solvent interaction is enhanced, while at the same time, the repulsion among first shell methanol molecules is also increased.²² Due to the balance of these two factors, the number of first shell methanol can be varied from 3 to 6, which produces only small changes (within 5 kcal/mol) in the total energy. As demonstrated in Tables 3 and 4, both the energetic values and the $\text{Mg}\cdots\text{H}$ (or $\text{Mg}\cdots\text{CH}_3$) distances for the two elimination channels are determined first and foremost by the number of first shell methanol. The presence of second shell methanol only produces minor changes.

For $\text{Mg}^+(\text{CH}_3\text{OH})_n$, the barrier for H elimination is still slightly higher than that for CH_3 elimination at $n = 5$, in contrast to a switch of the ordering observed for $\text{Ca}^+(\text{CH}_3\text{OH})_n$ at $n = 4$. It can be understood by the fact that for $\text{Mg}^+(\text{CH}_3\text{OH})_n$ the $\text{Mg}\cdots\text{H}$ interaction is actually stronger than the $\text{Mg}\cdots\text{CH}_3$ interactions for small n . In both channels, the interaction between the eliminated atom (or group) and the Mg ion become less effective, as the number of methanol increases, due to the “squeezing out” effect. Such a trend is also corroborated by the decrease in the energy required for the complete removal of H or CH_3 . This should be contrasted with the case of $\text{Ca}^+(\text{CH}_3\text{OH})_n$, in which the $\text{Ca}\cdots\text{CH}_3$ interaction is stronger and the “squeezing out” effect makes the CH_3 elimination less favorable.

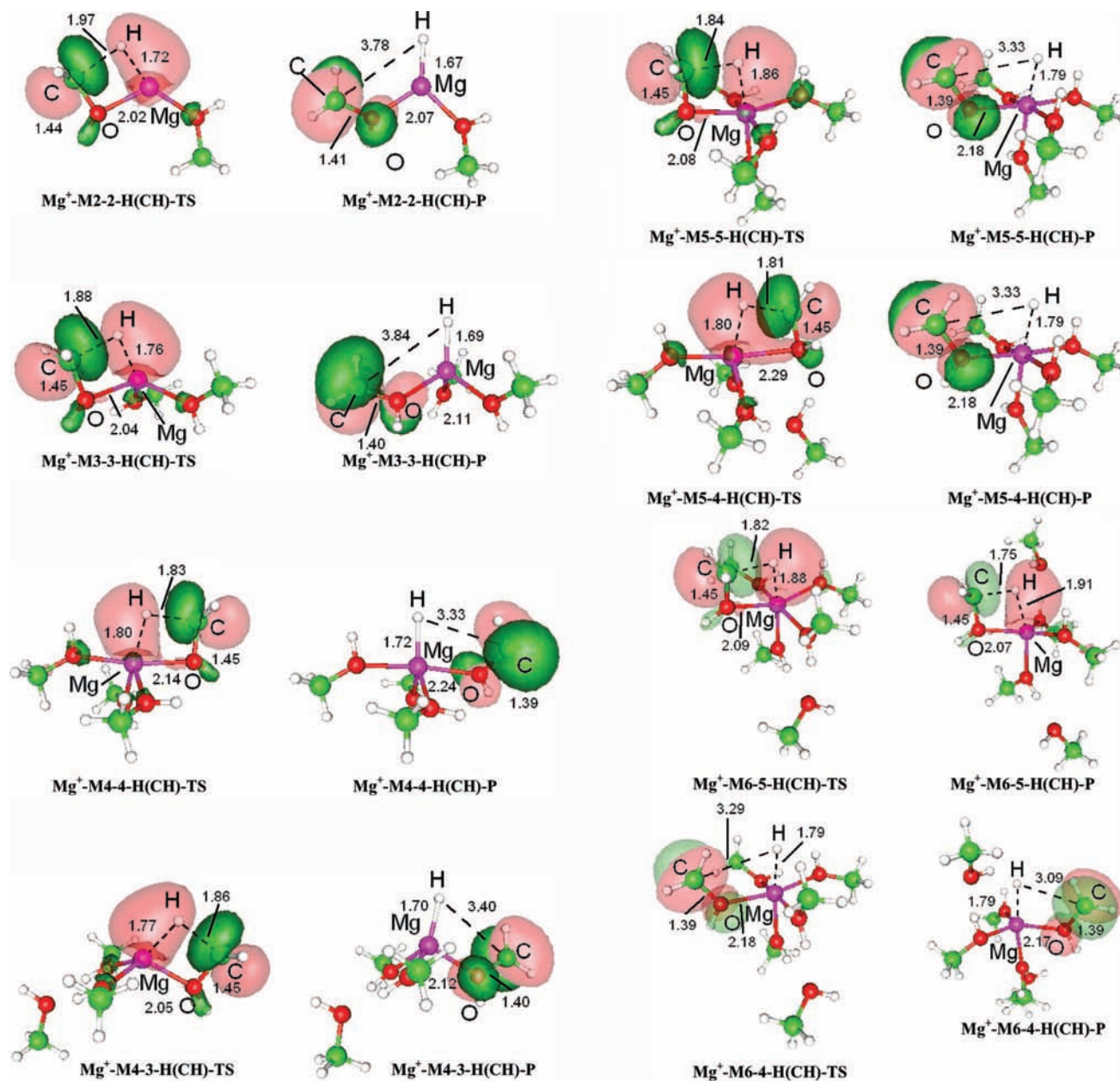


Figure 6. Transition and intermediate structures and their SOMO plots for the H(CH) elimination channel in $\text{Mg}^+(\text{CH}_3\text{OH})_n$.

TABLE 6: C–H Distances in Transition Structures, Energy Barriers, Reaction Energies, Mg–H Distances and Energies for Removing H from the Intermediates, for H(CH)-Elimination in $\text{Mg}^+(\text{CH}_3\text{OH})_n$, $n = 2-6$, Calculated at the B3LYP/6-311+G** Level^a

	$r(\text{C}-\text{H})$ (in Å)	energy barrier	reaction energy	$r(\text{Mg}-\text{H})$ (in Å)	energy for H removal
$\text{Mg}^+-\text{M2}-2$	1.97	44.5	33.5	1.67	37.2
$\text{Mg}^+-\text{M3}-3$	1.88	37.3	26.1	1.69	32.8
$\text{Mg}^+-\text{M4}-4$	1.83	31.8	23.0	1.72	22.1
$\text{Mg}^+-\text{M4}-3$	1.86	35.4	24.7	1.70	31.4
$\text{Mg}^+-\text{M5}-5$	1.84	29.8	20.5	1.79	27.0
$\text{Mg}^+-\text{M5}-4$	1.81	32.0	17.9	1.73	24.7
$\text{Mg}^+-\text{M6}-5$	1.82	28.1	19.2	1.79	26.7
$\text{Mg}^+-\text{M6}-4$	1.75	29.1	20.1	1.79	26.5

^a All energies are measured in kcal/mol and corrected for zero vibration.

At $n = 6$, a reversal is observed. When all six methanol molecules are in the first shell ($\text{Mg}^+-\text{M6}-6$), the barrier is 6.7

kcal/mol for H elimination and 9.6 kcal/mol for CH_3 elimination. Moreover, the CH_3 elimination barrier is also higher than the barrier of 7.2 kcal/mol for $\text{Mg}^+-\text{M5}-5$, reversing the trend of falling barrier with increasing cluster size. It is well understood that the maximum number of methanol molecules in the first shell is 6, and more importantly, $\text{Mg}^+-\text{M6}-6$ represents the closure of the first shell when the SOMO is detached from the Mg atom.²² It becomes a diffusive orbital distributed all over the six methanol molecules, which should be contrasted with the typical situation for $n \leq 5$, when the SOMO is an sp hybridized orbital on the Mg atom. In $\text{Mg}^+-\text{M6}-6$, the Mg ion can no longer play an assisting role in the breaking of O–H or O– CH_3 bonds. Furthermore, as the O–H bond is more polar than the O– CH_3 bond, the SOMO is distributed more on the O–H bond, which makes it easier for the transfer of this unpaired electron to a departing H atom. It explains the contrasting behavior for the two barriers going from $\text{Mg}^+-\text{M5}-5$ to $\text{Mg}^+-\text{M6}-6$, while the barrier for H elimination drops, the barrier for CH_3 elimination increases. It can be expected that

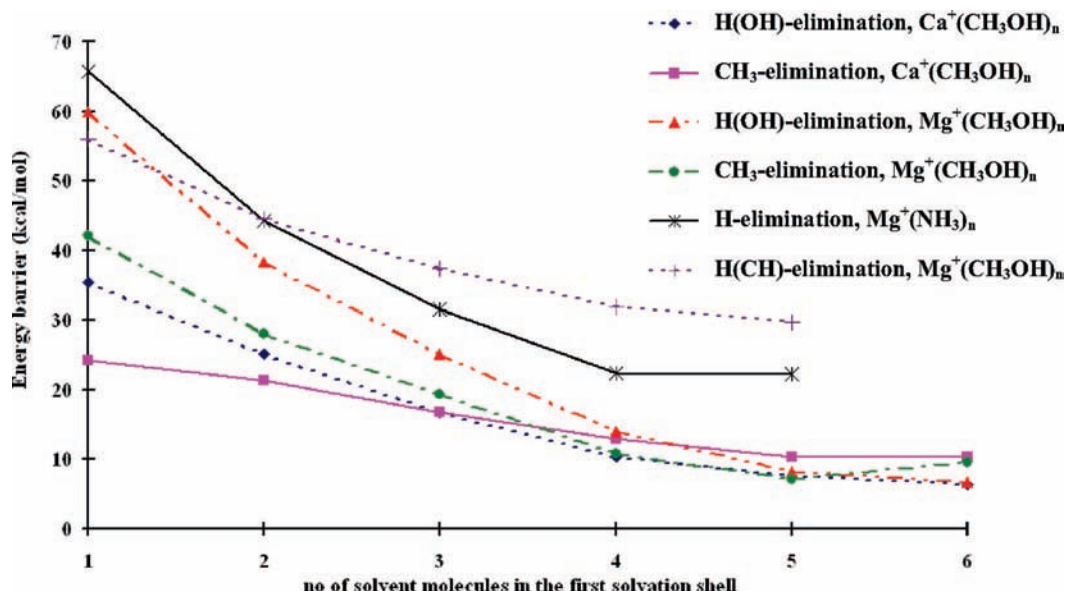


Figure 7. Energy barriers for all the reaction channels studied plotted against the number of solvent molecules in the first solvation shell.

for $n > 6$ the H elimination channel should be favored over the CH₃ channel, due to the detachment of the unpaired electron.

These results are in broad agreement with experimental observations. When n was in the range of 1–3, only CH₃ elimination was observed in collision induced dissociation,²⁵ whereas for n over 5, Lu and Yang reported that H elimination was the observed as the dominant channel.⁸

4. H (CH) Elimination for Mg⁺(CH₃OH)_n and H Elimination for Mg⁺(NH₃)_n. In the case of $n = 1$, the H (CH) elimination for Mg⁺(CH₃OH) and the H elimination for Mg⁺(NH₃) are actually similar to the H (OH) elimination, producing an intermediate structure stabilized by the bonding interaction between H and Mg ion. But the energy needed to break this bond is 55.2 kcal/mol for (H–MgOH–CH₂)⁺ and 40.4 kcal/mol for (H–MgNH₂)⁺, and considerably higher than the 29.3 kcal/mol for (H–MgOCH₃)⁺, all calculated at the CCSD/6-311+G** level. It has been pointed out that the interactions between Mg ion and OH=CH₂[–] and between Mg ion and NH₂[–] are less ionic, and compensated by a stronger Mg–H interaction.¹ Similar to the previously discussed elimination channels, the H atom should be squeezed out of the first shell and away from its direct interaction with Mg ion, as the cluster size grows, while the stronger Mg–H interaction in these two eliminations provides yet another interesting variation in the evolution of the elimination barrier.

For the ammonia clusters, the transition and intermediate structures are shown in Figure 5. The distance between H and Mg is 1.72 Å in Mg⁺-A2-2-H-P and 1.95 Å in Mg⁺-A5-5-H-P, which are comparable to the distance of 1.73 Å in Mg⁺-M2-2-H-P and 1.98 Å in Mg⁺-M5-5-H-P. However, the energy required for the removal of the H atom stays above 9 kcal/mol for all of the clusters studied as listed in Table 5. Both the reaction energy and barrier drop as n goes from 2 to 4. But beyond $n = 4$, the two quantities start to fluctuate. At a particular size, such as $n = 5$, these values also fluctuate when the solvent numbers in the first and second shells are varied. For all the reaction channels discussed in previous sections, the reaction energy and barrier fall as the number of first shell solvent molecules increases, as their interactions with the metal ion are more than enough to compensate for the elongation of metal···H distance. This is obviously not the case for Mg⁺(NH₃)_n, for which the reaction barrier stays above 20 kcal/mol when n reaches 5 and 6.

Neither is it for the H(CH) elimination in Mg⁺(CH₃OH)_n. As shown in Figure 6, the Mg···H distance in the intermediate structure starts at 1.67 Å at $n = 2$ for Mg⁺-M2-2-H(CH)-P, and increases to only 1.79 Å at $n = 5$ for Mg⁺-M5-5-H(CH)-P. The pace of increase is considerably slower than that for the H(OH) elimination or for the H elimination of Mg⁺(NH₃)_n. It indicates that the bonding interaction between H and Mg ion is strong, which makes it difficult to squeeze the H atom out. Indeed, the energy for breaking the Mg···H bond remains above 20 kcal/mol, as shown in Table 6. While the reaction energy falls to around an endothermic value of 20 kcal/mol, the elimination barrier is floored around 28 kcal/mol, despite the increase in the cluster size.

It should also be noted that for both channels we are unable to identify a transition structure for the cluster with all six solvent molecules in the first shell. By simply stretching an N–H bond in Mg⁺-A6-6, the energy required to break the N–H bond in Mg⁺(NH₃)₆ is 31 kcal/mol. Stretching the C–H bond in Mg⁺-M6-6 leads again to a Mg–H bond with a distance of 1.7 Å, but the barrier is ~42 kcal/mol. Tables 5 and 6 also indicate that the presence of second shell solvent molecules could lower the barrier and the reaction energy, although not by a significant amount.

The H elimination channel for Mg⁺(NH₃)_n and the H (CH) elimination channel for Mg⁺(CH₃OH) are quite different from the other elimination channels discussed in this paper. The interaction between the departing H and the metal ion is important in both the transition and the intermediate structure, which can not be completely compensated by the increasing number of solvent molecules in the first shell. As a result, the fall in the reaction barrier is floored around 20 kcal/mol for the H elimination channel in Mg⁺(NH₃)_n and 28 kcal/mol for the H (CH) elimination channel in Mg⁺(CH₃OH)_n. Both channels are not expected to be switched on with a growing cluster size, unless significant excitation energy is provided.

5. Conclusions

Reaction barrier is the key to understanding the elimination channels in the M⁺(L)_n clusters studied. The experimentally observed dominance of H elimination channel over the CH₃ elimination channel in both Ca⁺(L)_n and Mg⁺(L)_n with $n > 5$ is determined by the barrier, rather than the reaction energy.

Shown in Figure 7 is the reaction barrier for each of the studied elimination channel against the cluster size n . Overall, the barrier decreases as n increases, similar to the H elimination for $\text{Mg}^+(\text{H}_2\text{O})_n$, which can be explained by the stabilization effect of solvent molecules for the more polarizing ion core produced in these elimination channels.

However, except in the case of H(OH) elimination for $\text{Ca}^+(\text{CH}_3\text{OH})_n$, the metal ion plays an assistance role in all the other channels due to the bonding interaction between the departing H or CH_3 and the metal ion, especially for $n = 2$ and 3. As n increases further, this interaction is weakened as the H or CH_3 is squeezed out of the first solvation shell. When the unpaired electron is detached from the metal ion to form an ion pair, the H(OH) elimination channel is favored over the CH_3 elimination.

For the CH_3 elimination in $\text{Ca}^+(\text{CH}_3\text{OH})_n$, the H(OH) elimination in $\text{Mg}^+(\text{CH}_3\text{OH})_n$, and the CH_3 elimination in $\text{Mg}^+(\text{CH}_3\text{OH})_n$, the “squeezing out” effect is more than compensated by the stabilization of solvent molecules, and the reaction barrier can fall below 10 kcal/mol. For the H(CH) elimination in $\text{Mg}^+(\text{CH}_3\text{OH})_n$ and the H elimination in $\text{Mg}^+(\text{NH}_3)_n$, the interaction between Mg and H is very important and can not be easily compensated. As a result, their barriers flatten above 20 kcal/mol as n reaches 4 and above.

Acknowledgment. Calculations reported in this paper were performed on the computer clusters operated by the Department of Chemistry, the Chinese University of Hong Kong (CUHK), supported by a Special Equipment Grant, and on the SGI Origin 2000, at the Information Technology Services Center (ITSC), CUHK. We thank Mr. Ka Fai Woo at the Department of Chemistry and Mr. Frank Ng at ITSC for technical support. We gratefully acknowledge the financial support provided by the Hong Kong SAR Government, through the Project CUHK 401604P.

References and Notes

- (1) Chan, K. W.; Wu, Y.; Liu, Z. *J. Phys. Chem. A* **2008**, *112*, 8534.
- (2) Yoshida, S.; Daigoku, K.; Okai, N.; Takahata, A.; Sabu, A.; Hashimoto, K.; Fuke, K. *J. Chem. Phys.* **2002**, *117*, 8657.
- (3) Yoshida, S.; Okai, N.; Fuke, K. *Chem. Phys. Lett.* **2001**, *347*, 93.

- (4) Lee, J. I.; Sperry, D. C.; Farrar, J. M. *J. Chem. Phys.* **2001**, *114*, 6180.
- (5) Lee, J. I.; Sperry, D. C.; Farrar, J. M. *J. Chem. Phys.* **2004**, *121*, 8375.
- (6) Willey, K. F.; Yeh, C. S.; Robbins, D. L.; Pilgrim, J. S.; Duncan, M. A. *J. Chem. Phys.* **1992**, *97*, 8886.
- (7) Woodward, C. A.; Dobson, M. P.; Stace, A. J. *J. Phys. Chem. A* **1997**, *101*, 2279.
- (8) Lu, W. Y.; Yang, S. H. *J. Phys. Chem. A* **1998**, *102*, 825.
- (9) Farrar, J. M. *Int. Rev. Phys. Chem.* **2003**, *22*, 593.
- (10) Castleman, A. W., Jr.; Bowen, K. H. *J. Phys. Chem.* **1996**, *100*, 12911.
- (11) Fuke, K.; Hashimoto, K.; Iwata, S. *Adv. Chem. Phys.* **1999**, *110*, 431.
- (12) Harms, A. C.; Khanna, S. N.; Chen, A. B.; Castleman, A. W., Jr. *J. Chem. Phys.* **1994**, *100*, 3540.
- (13) Sanekata, M.; Misaizu, F.; Fuke, K.; Iwata, S.; Hashimoto, K. *J. Am. Chem. Soc.* **1995**, *117*, 747.
- (14) Berg, C.; Beyer, M.; Achatz, U.; Joos, S.; Niedner-Schatteburg, G.; Bondybey, V. E. *Chem. Phys.* **1998**, *239*, 379.
- (15) Siu, C. K.; Liu, Z. F. *Chem. Eu. J.* **2002**, *8*, 3177.
- (16) Siu, C. K.; Liu, Z. F. *Phys. Chem. Chem. Phys.* **2005**, *7*, 1005.
- (17) Watanabe, H.; Iwata, S.; Hashimoto, K.; Misaizu, F.; Fuke, K. *J. Am. Chem. Soc.* **1995**, *117*, 755.
- (18) Reinhard, B. M.; Niedner-Schatteburg, G. *J. Chem. Phys.* **2003**, *118*, 3571.
- (19) Reinhard, B. M.; Niedner-Schatteburg, G. *Phys. Chem. Chem. Phys.* **2002**, *4*, 1471.
- (20) Watanabe, H.; Iwata, S. *J. Phys. Chem. A* **1997**, *101*, 487.
- (21) Chan, K. W.; Siu, C. K.; Wong, S. Y.; Liu, Z. F. *J. Chem. Phys.* **2005**, *123*, 124313.
- (22) Chan, K. W.; Wu, Y.; Liu, Z. *Can. J. Chem.* **2007**, *85*, 873.
- (23) Frisch, M. J.; Trucks, G. W.; Schlegel, H. B.; Scuseria, G. E.; Robb, M. A.; Cheeseman, J. R.; Zakrzewski, V. G.; Montgomery, J. A.; Stratmann, R. E.; Burant, J. C.; Dapprich, S.; Millam, J. M.; Daniels, A. D.; Kudin, K. N.; Strain, M. C.; Farkas, O.; Tomasi, J.; Barone, V.; Cossi, M.; Cammi, R.; Mennucci, B.; Pomelli, C.; Adamo, C.; Clifford, S.; Ochterski, J.; Petersson, G. A.; Ayala, P. Y.; Cui, Q.; Morokuma, K.; Malick, D. K.; Rabuck, A. D.; Raghavachari, K.; Foresman, J. B.; Cioslowski, J.; Ortiz, J. V.; Stefanov, B. B.; Liu, G.; Liashenko, A.; Piskorz, P.; Komaromi, I.; Gomperts, R.; Martin, R. L.; Fox, D. J.; Keith, T.; Al-Laham, M. A.; Peng, C. Y.; Nanayakkara, A.; Gonzalez, C.; Challacombe, M.; Gill, P. M. W.; Johnson, B.; Chen, W.; Wong, M. W.; Andres, J. L.; Gonzalez, C.; Head-Gordon, M.; Replogle, E. S.; Pople, J. A. *Gaussian 98*, revision A.11; Gaussian, Inc.: Pittsburgh, PA, 1998.
- (24) Lide, D. R., Ed.; *CRC Handbook of Chemistry and Physics*, 77th ed.; CRC Press: Boca Raton, FL, 1997.
- (25) Andersen, A.; Muntean, F.; Walter, D.; Rue, C.; Armentrout, P. B. *J. Phys. Chem. A* **2000**, *104*, 692.

JP804156F